Verification of complementarity relations between quantum steering criteria using an optical system

Huan Yang,[1,2,3] Zhi-Yong Ding,[1,4,5] Xue-Ke Song,[1] Hao Yuan,[1,6,7] Dong Wang,[1,6] Jie Yang,[1] Chang-Jin Zhang,[1,3] and Liu Ye[1,*]

[1]*School of Physics and Material Science, Anhui University, Hefei 230601, China*
[2]*Department of Experiment and Practical Training Management, West Anhui University, Lu'an 237012, China*
[3]*Institute of Physical Science and Information Technology, Anhui University, Hefei 230601, China*
[4]*School of Physics and Electronic Engineering, Fuyang Normal University, Fuyang 236037, China*
[5]*Key Laboratory of Functional Materials and Devices for Informatics of Anhui Educational Institutions, Fuyang Normal University, Fuyang 236037, China*
[6]*CAS Key Laboratory of Quantum Information, University of Science and Technology of China, Hefei 230026, China*
[7]*Key Laboratory of Opto-Electronic Information Acquisition and Manipulation of Ministry of Education, Anhui University, Hefei 230601, China*

(Received 27 July 2020; revised 18 January 2021; accepted 28 January 2021; published 10 February 2021)

The ability that one system immediately affects another one by using local measurements is regarded as quantum steering, which can be detected by various steering criteria. Recently, Mondal *et al.* [Phys. Rev. A **98**, 052330 (2018)] derived the complementarity relations of coherence steering criteria, and revealed that the quantum steering of a system can be observed through the average coherence of a subsystem. Here, we experimentally verify the complementarity relations between quantum steering criteria by employing two-photon Bell-like states and three Pauli operators. The results demonstrate that if prepared quantum states can violate two setting coherence steering criteria and turn out to be steerable states, then they cannot violate the complementary settings criteria. Three measurement settings inequalities, which establish a set of complementarity relations between these two coherence steering criteria, are always obeyed by all prepared quantum states in experiment. In addition, we experimentally certify that the strengths of coherence steering criteria depend on the choice of coherence measure. In comparison with two setting coherence steering criteria based on l_1 norm of coherence and relative entropy of coherence, our experimental results show that the steering criterion based on skew information of coherence is the strongest in detecting the steerability of two-photon Bell-like states. Thus, our experimental demonstration can deepen the understanding of the relation between the quantum steering and quantum coherence.

DOI: 10.1103/PhysRevA.103.022207

I. INTRODUCTION

Quantum steering describes a nontrivial trait of the quantum world that one subsystem of bipartite systems can instantaneously affect another one by using local measurements [1,2]. In contrast to the entanglement [3] and Bell nonlocality [4,5], quantum steering was only rigorously and formally defined from the perspective of quantum information theory in 2007 [6], subsequently, it has been attracting extensive attention in different fields [7]. The detection of quantum steering can be realized through the violations of steering criteria (also called steering inequalities), which can be obtained by using correlations, state assemblages, and full information [7]. There are various steering criteria, including linear and nonlinear steering criteria [8,9], steering inequality from uncertainty relations [10–13], steering criterion from geometric Bell-like inequality [14], steering inequalities from semidefinite programs [15], and full information steering inequality [16]. So far, quantum steering embodies vital application values in subchannel discrimination, resource theory of steering, quantum communication, quantum teleportation, randomness generation, and so on [7]. Also, it has been demonstrated in a series of significant experiments [17–26].

Coherence, which originates from the superposition principle of quantum mechanics, reflects one of the fundamental essences in many quantum phenomena [27,28]. Although the investigations concerning coherence have a long-standing history, the rigorous quantification of coherence in the field of quantum information has never been established. Until 2014, based on incoherent operations, Baumgratz *et al.* [29] put forward the general frame of quantifying coherence for quantum states, and this quantification relies on a fixed reference basis. One can measure quantum coherence via l_1 norm of coherence (l_1C) [29], relative entropy of coherence (REC) [29], robustness of coherence [30,31], and skew information of coherence (SIC) [32–34]. Recently, quantum coherence has become a hot topic in both theory [35–40] and experiment [41–44]. It plays a central part in different fields, such as quantum metrology, quantum thermodynamics, quantum algorithms, and quantum channel discrimination [27].

The concept of complementarity describes that two quantum observables of quantum mechanics cannot be measured simultaneously [45]. Notably, it is a new tendency for

*yeliu@ahu.edu.cn

establishing the complementarity relations of different physical quantities in quantum information theory. According to these complementary relations, one can establish a bound on a quantity via another complementary quantity, and can also deeply understand the correlation between these complementary quantities. There are several promising efforts in concerning fields [46–53]. Singh *et al.* [46] obtained a complementarity relation between maximal coherence and mixedness, and examined the limitation of a system's mixedness on the quantum coherence. Their results revealed that the upper bound of maximum coherence of a quantum state can be obtained through its complementary quantity, i.e., the mixedness. Since the noise of the external environment can enhance the mixedness of the state, this complementary relation is also beneficial to understand the interplay between coherence and noise [46]. Cheng and Hall [47] explored complementarity relations between the coherences of mutually unbiased bases, and derived relations among coherence, purity, and uncertainty. Considering the maximal violations of the Clauser-Horne-Shimony-Holt inequality, the trade-off relations of Bell violations among pairwise qubit systems were investigated by Qin *et al.* [48], and the relations constrain the distribution of nonlocality among the subsystems. By using the REC, Sharma and Pati [49] presented the trade-off relation between the system's coherence and disturbance induced by a completely positive trace-preserving map. For a multipartite system, the trade-off relations for tripartite nonlocality were established by Zhao *et al.* [50]. Experimentally, different complementarity and trade-off relations were also tested [54–56]. By employing a photonic qutrit-qubit hybrid system, Zhan *et al.* [54] experimentally verified the contextuality-nonlocality trade-off relation, and the results certified that entanglement is a particular form for a fundamental quantum resource. Weston *et al.* [55] experimentally tested the universal complementarity relations satisfied by any joint measurement of two observables. In two noncommuting reference bases, Lv *et al.* [56] experimentally verified the trade-off relation of quantum coherence, and their results displayed that the lower and upper bounds restrict the sum of quantum coherence under these bases.

Recently, Mondal *et al.* [57] obtained the complementarity relations between coherence steering criteria by employing different quantifications of quantum coherence. This work established a connection between two valuable quantum resources in quantum information task, i.e., quantum steering and quantum coherence. However, the test of the complementarity relations in experiment is still lacking. The present investigation may further deepen our understanding of the relation between the quantum steering and quantum coherence in practice. Also, it can demonstrate a method to detect quantum steering in experiment, namely, one can witness quantum steering of the system via detecting the quantum coherence of the subsystem. Motivated by this, we experimentally verify the complementarity relations between different coherence steering criteria in this work. The experimental results show that one setting coherence steering criteria cannot be violated if its complementary criteria can be violated by prepared quantum states. In comparison with two setting coherence steering criteria from l_1C and REC, the prepared states more easily violate two setting coherence steering criterion based on SIC, suggesting that it can detect more steerable Bell-like states in experiment.

II. COHERENCE STEERING CRITERIA AND COMPLEMENTARITY RELATIONS

An entangled state ρ_{AB} is prepared by Alice. And then, the system B is sent to Bob. The task of Alice is to make Bob believe the fact that the state shared by them is indeed entangled, hence, the nonlocal correlation is shared by them. However, Bob does not trust Alice and only considers the system B is quantum. Also, Bob thinks that Alice may use a single quantum system B to cheat him [17]. If and only if the state of Bob cannot be represented by using the local hidden state (LHS) model [6] $\rho_a^A = \sum_\lambda p(\lambda)p(a|A,\lambda)\rho_B^Q(\lambda)$, then Bob accepts the fact that the ρ_{AB} prepared by Alice is an entangled state, and nonlocal correlation is shared by them. Here, λ is a hidden variable with $\sum_\lambda p(\lambda) = 1$, and $\rho_B^Q(\lambda)$ is LHS. $\{p(\lambda), \rho_B^Q(\lambda)\}$ denotes an ensemble of preexisting LHSs for Bob, and $p(a|A,\lambda)$ indicates the stochastic map of Alice, which is used to convince or fool Bob via ρ_a^A. The ρ_{AB} is a steerable state if and only if the joint probabilities of measurement outcomes (Alice performs the measurement A on her subsystem and obtains the outcome $a \in \{0, 1\}$; Bob performs the measurement B and obtains the outcome $b \in \{0, 1\}$) cannot be described by employing a local hidden variable–local hidden state (LHV-LHS) model, namely, $P(a, b|A, B, \rho_{AB}) = \sum_\lambda P(\lambda)P(a|A,\lambda)P_Q(b|B,\rho_\lambda)$, where $P_Q(b|B,\rho_\lambda)$ is the probability of the outcome b corresponding to measurement B.

In 2018, Mondal and Kaszlikowski [57] proposed the coherence steering criteria, which can help us to observe the quantum steering of a two-qubit state via the quantum coherence of the subsystem. For two-qubit states $\rho_{AB} = (\mathbb{I}\otimes\mathbb{I} + \mathbf{r}\cdot\boldsymbol{\sigma}\otimes\mathbb{I} + \mathbb{I}\otimes\mathbf{s}\cdot\boldsymbol{\sigma} + \sum_{i,j} t_{ij}\sigma_i\otimes\sigma_j)/4$ and three Pauli operators $\{\sigma_i\}$ $(i = x, y, z)$ as a complete set of mutually unbiased bases (MUBs), where $\mathbf{r} = \mathrm{tr}(\rho_{AB}\boldsymbol{\sigma}\otimes\mathbb{I})$, $\mathbf{s} = \mathrm{tr}(\rho_{AB}\mathbb{I}\otimes\boldsymbol{\sigma})$, and $t_{ij} = \mathrm{tr}(\rho_{AB}\sigma_i\otimes\sigma_j)$, Alice implements a projective measurement on her system by using the eigenbasis of σ_i and the corresponding outcome is $a \in \{0, 1\}$. The corresponding probability is $p(\rho_{B|M_a^i}) = \mathrm{tr}[(M_a^i\otimes\mathbb{I})\rho_{AB}]$, and the measurement operator is $M_a^i = [\mathbb{I} + (-1)^a\sigma_i]/2$. Similarly, Alice can measure her system by employing another measurement operator $M_a^k = [\mathbb{I} + (-1)^a\sigma_k]/2$, and $k \neq i$, $k \in \{x, y, z\}$. For each projective measurement implemented by Alice, Bob can measure the coherence of his conditional state $\rho_{B|M_a^i}$ under the eigenbasis of every Pauli operator. According to the number of Pauli operators chosen by Bob, the coherence steering criteria can be divided into one measurement setting (or one setting) and two measurement settings (or two setting), respectively [57]. Explicitly, the probability superposition of coherences of $\rho_{B|M_a^i}$ can be defined as

$$S_\ell^B(\rho_{AB}) = \sum_{i,a} p\big(\rho_{B|M_a^i}\big)C_{i+\ell}^q\big(\rho_{B|M_a^i}\big), \tag{1}$$

where $\ell \in \{0, 1, 2\}$, $C_i^q(\rho)$ represents different coherence measures under the eigenbasis of Pauli operator σ_i, including l_1C [$q = l_1$C and $C_i^{l_1\mathrm{C}}(\rho) = \sum_{i\neq j}|\langle k_i|\rho|k_j\rangle|$], REC

[q = REC and $C_i^{\mathrm{REC}}(\rho) = S(\rho^{\mathrm{diag}}) - S(\rho)$], and SIC [$q$ = SIC and $C_i^{\mathrm{SIC}}(\rho) = -(\mathrm{tr}[\sqrt{\rho}, \sigma_i]^2)/2$]. $\{|k_i\rangle, |k_j\rangle\}$ denote the eigenvectors of σ_i, $S(x)$ is the von Neumann entropy, and $\rho^{\mathrm{diag}} = \sum_i |k_i\rangle\langle k_i|\rho|k_i\rangle\langle k_i|$. If Bob measures the coherence only in one Pauli operator σ_i, which is the same as each projective measurement chosen by Alice (i.e., $\ell = 0$), then the one setting coherence steering criteria are given by

$$S_0^B(\rho_{AB}) = \sum_{i,a} p\left(\rho_{B|M_a^i}\right) C_i^q\left(\rho_{B|M_a^i}\right) \leqslant \varepsilon^q. \tag{2}$$

Here, $q \in \{l_1\mathrm{C}, \mathrm{REC}, \mathrm{SIC}\}$ indicates different coherence measures, $\varepsilon^q \in \{\sqrt{6}, 2.23, 2\}$ [51] represents the upper bounds of quantum coherence measured in a complete set of MUBs for a single-qubit state, and the quantum coherence of any single-qubit state cannot puncture the bounds. The violation of the criteria means that the ρ_{AB} is a steerable state. If Bob measures the coherence in the eigenbasis of another two Pauli operators σ_j and σ_k ($j \neq k \neq i$) (corresponding to $\ell = 1, 2$), which are different from the one chosen by Alice's measurement, there exists the two setting coherence steering criteria

$$\tfrac{1}{2} S_{12}^B(\rho_{AB}) = \tfrac{1}{2}\left[S_1^B(\rho_{AB}) + S_2^B(\rho_{AB})\right] \leqslant \varepsilon^q. \tag{3}$$

Bob's conditional state with the LHS model obeys these steering criteria. For a bipartite state, by performing local measurements on subsystem Alice, the average coherence of the conditional state of subsystem Bob summing over the MUBs [i.e., the left side of Eq. (3)] can puncture the upper bounds ε^q. This phenomenon is termed as the nonlocal advantage of quantum coherence (NAQC), and any two-qubit state that can achieve NAQC is not only entangled but also steerable [51]. Also, there are some steerable states which cannot achieve NAQC, and the average coherence of Bob's system can certify the steerability of bipartite states [51,57]. The violation of the criteria means that the ρ_{AB} is steerable. If Bob measures the coherence under the eigenbasis of three Pauli operators after each projective measurement performed by Alice on her subsystem, the inequality of three measurement settings is

$$\tfrac{1}{3} S_{012}^B(\rho_{AB}) = \tfrac{1}{3}\left[S_0^B(\rho_{AB}) + S_1^B(\rho_{AB}) + S_2^B(\rho_{AB})\right] \leqslant \varepsilon^q. \tag{4}$$

The LHS model of Bob's conditional state is not used in the derivation of Eq. (4) [57], and all two-qubit states ρ_{AB} satisfy Eq. (4). For this reason, the inequality of three measurement settings cannot be used to detect the quantum steering of ρ_{AB}. In reality, Eq. (4) describes a set of complementarity relations between one setting coherence steering criteria and two setting coherence steering criteria, that is,

$$\tfrac{1}{3} S_{012}^B(\rho_{AB}) = \tfrac{1}{3}\left[S_0^B(\rho_{AB}) + S_{12}^B(\rho_{AB})\right] \leqslant \varepsilon^q. \tag{5}$$

The results manifest that if one criterion between Eqs. (2) and (3) is violated, then the other one as a compensation can never be violated.

III. EXPERIMENTAL DEMONSTRATION AND RESULTS

In the process of our experimental implementation, we choose two-photon Bell-like states as test states. The polarized photons are encoded as qubits. The horizontally and vertically polarized states are described by using $|H\rangle$ and $|V\rangle$, respectively. Hence, two-photon Bell-like states are $\rho_{AB} = |\phi_{AB}\rangle\langle\phi_{AB}|$ with $|\phi_{AB}\rangle = \cos\theta|HH\rangle + \sin\theta|VV\rangle$.

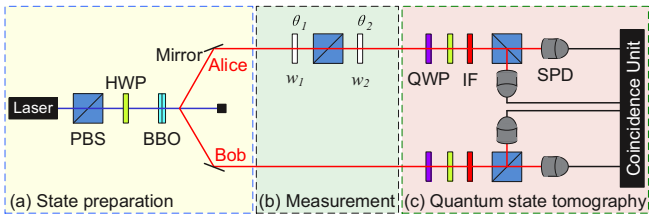

FIG. 1. Experimental setup. The module (a) is used to prepare two-photon Bell-like states. Module (b) is used to achieve six PMOs on Alice's photon. The first role of module (c) is used to perform the tomography on quantum states. The second role of module (c) is to implement six PMOs on the photons of Alice and Bob, which is used to carry out a steering inequality test for prepared two-photon Bell-like states. PBS, polarizing beam splitter; HWP, half-wave plate; BBO, type-I β-barium borate; QWP, quarter-wave plate; IF: interference filter; SPD: single-photon detector. w_1 and w_2: the types of wave plates; θ_1 and θ_2: the angles of optical axes of wave plates.

Figure 1 provides the schematic diagram of an all-optical experiment setup which is used to realize the verification of the complementarity relations. The setup contains three modules. The yellow area is the module (a) to prepare test states. To be explicit, high-power continuous pumped beam (the power is 130 mW and the wavelength is 405 nm) passes through the polarization beam splitter (PBS). The state of pumped beam transforms into the horizontally polarized state $|H\rangle$. This light beam first passes through the half-wave plate (HWP), and then is focused on two type-I β-barium borate (BBO) crystals ($6.0 \times 6.0 \times 0.5$ mm^3, and the optical axis is cut at 29.2°). Under the spontaneous parametric down conversion [58], Bell-like states $|\phi_{AB}\rangle = \cos\theta|HH\rangle + \sin\theta|VV\rangle$ shared by a pair of entangled photons (the central wavelength is 810 nm) are prepared. The state parameter θ can be easily changed by controlling the angle of optical axis of the HWP. Experimentally, we set θ to 0°, 10°, 20°, 30°, 40°, 45°, 50°, 60°, 70°, 80°, and 90°, respectively. The average fidelity of these test states is $\bar{F} = 0.9986 \pm 0.0042$, which is obtained according to $F(\rho, \rho_{\mathrm{theor}}) \equiv \mathrm{Tr}\sqrt{\sqrt{\rho}\rho_{\mathrm{theor}}\sqrt{\rho}}$ [59]. Here, the theoretical and experimental density matrices are indicated by ρ_{theor} and ρ, respectively. We estimate the error bars according to the statistical variation of coincidence counts obeyed by the Poisson distribution [60]. In order to experimentally demonstrate the complementarity relations between quantum steering criteria in Ref. [57], we need to realize a complete set of MUB measurements. In our experiment, we choose $X = \{|D\rangle\langle D|, |A\rangle\langle A|\}$, $Y = \{|R\rangle\langle R|, |L\rangle\langle L|\}$, and $Z = \{|H\rangle\langle H|, |V\rangle\langle V|\}$ as a complete set of MUB

TABLE I. The settings of wave plates in the module [Fig. 1(b)] for realizing different PMOs on the photon of Alice.

Settings	M_0^x	M_1^x	M_0^y	M_1^y	M_0^z	M_1^z
w_1	HWP	HWP	QWP	QWP	HWP	HWP
θ_1	22.5°	−22.5°	45°	−45°	0°	45°
w_2	HWP	HWP	QWP	QWP	HWP	HWP
θ_2	22.5°	−22.5°	−45°	45°	0°	45°

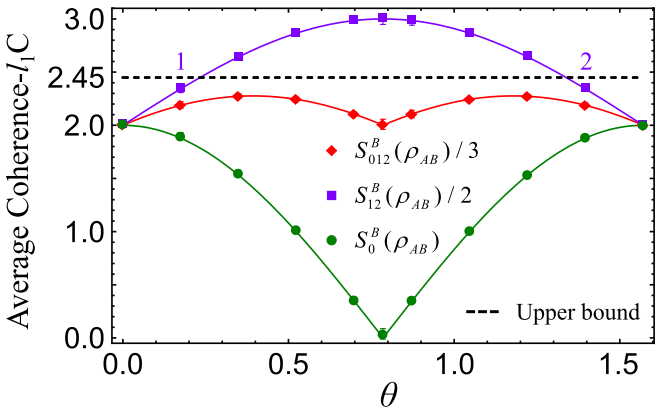

FIG. 2. Experimental results of the l_1C. The red rhombuses indicate the experimental results of $S^B_{012}(\rho_{AB})/3$, the purple squares denote the experimental results of $S^B_{12}(\rho_{AB})/2$, and the green solid circles represent the experimental results of $S^B_0(\rho_{AB})$. The corresponding theoretical predictions are represented by using solid lines with different colors. The black dashed line represents the upper bound $\varepsilon^{l_1\mathrm{C}} = \sqrt{6}$.

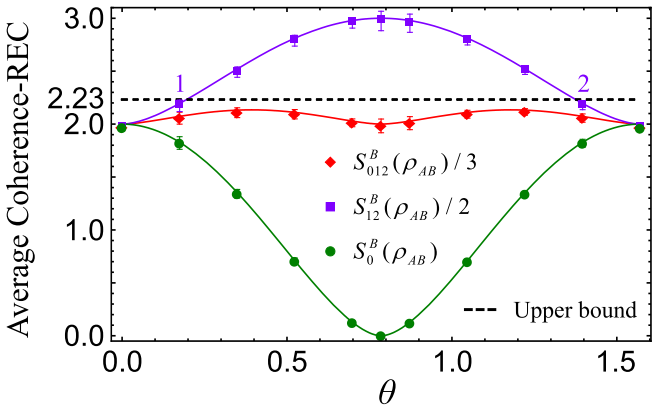

FIG. 3. Experimental results of the REC. The red rhombuses indicate the experimental results of $S^B_{012}(\rho_{AB})/3$, the purple squares denote the experimental results of $S^B_{12}(\rho_{AB})/2$, and the green solid circles represent the experimental results of $S^B_0(\rho_{AB})$. The corresponding theoretical predictions are represented by employing solid lines with different colors. The black dashed line represents the upper bound $\varepsilon^{\mathrm{REC}} = 2.23$.

measurements. Here, $\{|D\rangle = (|H\rangle + |V\rangle)/\sqrt{2}, |A\rangle = (|H\rangle - |V\rangle)/\sqrt{2}\}$, $\{|R\rangle = (|H\rangle + i|V\rangle)/\sqrt{2}, |L\rangle = (|H\rangle - i|V\rangle)/\sqrt{2}\}$, and $\{|H\rangle, |V\rangle\}$ are eigenvectors of σ_x, σ_y, and σ_z, respectively. For simplicity, we use $M^x_0 = |D\rangle\langle D|$, $M^x_1 = |A\rangle\langle A|$, $M^y_0 = |R\rangle\langle R|$, $M^y_1 = |L\rangle\langle L|$, $M^z_0 = |H\rangle\langle H|$, and $M^z_1 = |V\rangle\langle V|$ to represent six projection measurement operators (PMOs). In this work, the six PMOs implemented on Alice's photon can be realized in the module [Fig. 1(b)]. This module consists of two wave plates (denoted by w_1 and w_2; the rotation angles of the optical axes for w_1 and w_2 are denoted by θ_1 and θ_2, respectively) and a PBS. The six PMOs can be realized by adjusting the types and angles of the two wave plates in the module [Fig. 1(b)], as shown in Table I. The density matrices of states can be reconstructed through the quantum state tomography [61,62] in the module [Fig. 1(c)] (as the pink area displayed in Fig. 1). Beyond this, the module [Fig. 1(c)] can also be used to implement a steering inequality test for prepared two-photon Bell-like states. Of particular note, consider the scenario of quantum steering; in order to observe quantum steering of Bell-like states by using the coherence steering criteria, the experiment would need to be altered such that Alice does not need to be trusted. That is to say, one can remove the module [Fig. 1(b)]; the wave plates and PBS of Alice's side in the module [Fig. 1(c)] are used to realize different PMOs and obtain the corresponding measurement outcomes; the wave plates and PBS of Bob's side in the module [Fig. 1(c)] are used to implement single-qubit tomography and attain corresponding Bob's states (with his state conditioned on Alice's measurement setting and outcome).

Now let us turn to verify the complementarity relations between quantum steering criteria in experiment. The experimental measurement probabilities $p(\rho_{B|M^i_a})$ in Eqs. (2)–(4) are obtained by virtue of coincidence counts [63], and the corresponding coherence $C^q_i(\rho_{B|M^i_a})$ are calculated according to the density matrices of states restructured via quantum state tomography. Thus, the experimental results of $S^B_0(\rho_{AB})$, $S^B_{12}(\rho_{AB})/2$, and $S^B_{012}(\rho_{AB})/3$ can be attained in different coherence measures. In detail, Fig. 2 and Table II depict the results based on l_1C. Figure 3 and Table III provide the results based on REC. The results

TABLE II. Experimental data of $S^B_{012}(\rho_{AB})/3$, $S^B_{12}(\rho_{AB})/2$, and $S^B_0(\rho_{AB})$ based on the l_1C.

θ	$S^B_{012}(\rho_{AB})/3$	$S^B_{12}(\rho_{AB})/2$	$S^B_0(\rho_{AB})$
0°	2.006 ± 0.020	2.002 ± 0.020	2.015 ± 0.019
10°	2.192 ± 0.031	2.338 ± 0.030	1.899 ± 0.032
20°	2.275 ± 0.020	2.637 ± 0.017	1.550 ± 0.025
30°	2.247 ± 0.017	2.862 ± 0.015	1.019 ± 0.022
40°	2.107 ± 0.017	2.981 ± 0.013	0.358 ± 0.024
45°	2.010 ± 0.047	2.995 ± 0.047	0.038 ± 0.049
50°	2.106 ± 0.036	2.981 ± 0.039	0.356 ± 0.029
60°	2.245 ± 0.015	2.863 ± 0.012	1.010 ± 0.022
70°	2.274 ± 0.014	2.642 ± 0.011	1.537 ± 0.019
80°	2.189 ± 0.021	2.340 ± 0.021	1.888 ± 0.020
90°	2.002 ± 0.015	2.001 ± 0.016	2.004 ± 0.015

TABLE III. Experimental data of $S^B_{012}(\rho_{AB})/3$, $S^B_{12}(\rho_{AB})/2$, and $S^B_0(\rho_{AB})$ based on the REC.

θ	$S^B_{012}(\rho_{AB})/3$	$S^B_{12}(\rho_{AB})/2$	$S^B_0(\rho_{AB})$
0°	1.968 ± 0.024	1.969 ± 0.020	1.967 ± 0.032
10°	2.056 ± 0.057	2.173 ± 0.055	1.821 ± 0.060
20°	2.108 ± 0.046	2.491 ± 0.049	1.342 ± 0.041
30°	2.093 ± 0.044	2.788 ± 0.051	0.704 ± 0.030
40°	2.012 ± 0.037	2.955 ± 0.048	0.125 ± 0.014
45°	1.983 ± 0.065	2.974 ± 0.092	0.002 ± 0.011
50°	2.009 ± 0.062	2.953 ± 0.086	0.120 ± 0.014
60°	2.093 ± 0.037	2.790 ± 0.042	0.700 ± 0.026
70°	2.115 ± 0.031	2.503 ± 0.033	1.339 ± 0.026
80°	2.057 ± 0.039	2.176 ± 0.040	1.819 ± 0.038
90°	1.966 ± 0.015	1.968 ± 0.013	1.961 ± 0.020

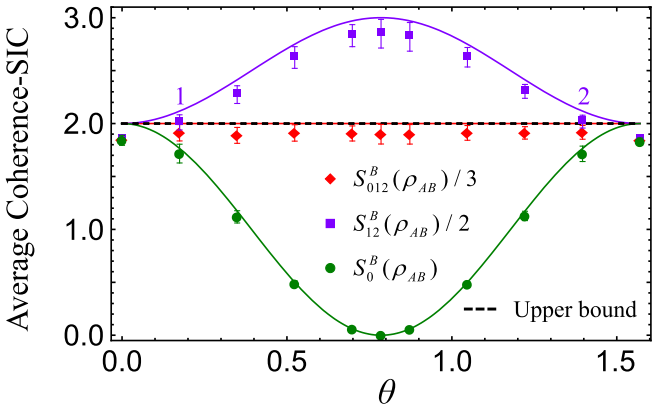

FIG. 4. Experimental results of SIC. The red rhombuses indicate the experimental results of $S^B_{012}(\rho_{AB})/3$, the purple squares denote the experimental results of $S^B_{12}(\rho_{AB})/2$, and the green solid circles represent the experimental results of $S^B_0(\rho_{AB})$. The corresponding theoretical predictions are represented by using solid lines with different colors. The black dashed line represents the upper bound $\varepsilon^{\mathrm{SIC}} = 2$.

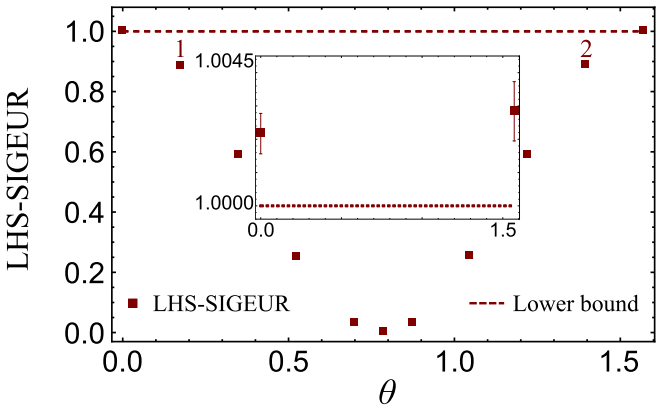

FIG. 5. Experimental results of LHS-SIGEUR for prepared Bell-like states. The inset represents the magnifications of the experimental results for Bell-like states with $\theta = 0^\circ$ and $\theta = 90^\circ$.

based on SIC are depicted in Fig. 4 and Table IV. The error bars in Figs. 2–5 and Tables II–IV, and VI represent one standard deviation, and mainly originate from the fluctuation of the statistical distribution of photons. Hence, for each quantity, we use the subprogram of Poisson distribution in *Mathematica* 11.0 to randomly generate 100 grouped coincidence counts. The error bar of this quantity is estimated according to the standard deviation. It is worthwhile to note that some of the error bars are too short to exhibit in Figs. 2–4. For all figures, the green solid circles, purple squares, and red rhombuses denote the experimental results of $S^B_0(\rho_{AB})$, $S^B_{12}(\rho_{AB})/2$, and $S^B_{012}(\rho_{AB})/3$, respectively. The corresponding theoretical results are displayed by means of different colored curves, and the black dashed lines are the upper bounds $\varepsilon^q (q = l_1\mathrm{C}, \mathrm{REC}, \mathrm{SIC})$ in Eqs. (2)–(4). As displayed from Figs. 2–4, the experimental results are in good agreement with the theoretical predictions. No matter what kind of coherence measure is chosen, the experimental results of $S^B_0(\rho_{AB})$ are anticorrelated with those of $S^B_{12}(\rho_{AB})/2$. Moreover, the experimental results certify that if two setting coherence steering criteria are violated $[S^B_{12}(\rho_{AB})/2 > \varepsilon^q]$ by prepared Bell-like states, then one setting coherence steering criteria as compensations cannot be violated $[S^B_0(\rho_{AB}) \leqslant \varepsilon^q]$ by these states. All prepared Bell-like states cannot violate three measurement settings inequalities $[S^B_{012}(\rho_{AB})/3 \leqslant \varepsilon^q]$.

From Figs. 2–4 and Tables II–IV, one can find that seven prepared Bell-like states ($\theta = 20^\circ, 30^\circ, 40^\circ, 45^\circ, 50^\circ, 60^\circ, 70^\circ$) can violate two setting coherence steering criteria based on different coherence measures (i.e., l_1C, REC, and SIC). For these states, the experimental average coherence of Bob's conditional states can puncture the upper bounds ε^q that cannot be punctured by any single-qubit state. The results demonstrate that these seven prepared Bell-like states are steerable states. It also deserves emphasizing that two prepared Bell-like states with $\theta = 10^\circ$ and $\theta = 80^\circ$ (labeled by 1 and 2 in Figs. 2–4, respectively) can violate two setting coherence steering criterion based on SIC. However, these two states cannot violate the criteria based on l_1C and REC. The experimental results verify that the quantum steering of these two states can only be detected by the two setting coherence steering criterion based on SIC, and cannot be captured through the ones based on l_1C and REC. In order to further certify the advantage of the two setting coherence steering criterion based on SIC in detecting the steerability of Bell-like states with $\theta = 10^\circ$ and $\theta = 80^\circ$, we perform a steering inequality test on all prepared states by using steering inequality from the general entropic uncertainty relation (SIGEUR), which is an effective tool to detect quantum steering [12,25,26]. The SIGEUR is written as $(n-1)^{-1}\sum_i\{1-\sum_{ab}[(p^{(i)}_{ab})^n/(p^{(i)}_a)^{n-1}]\} \geqslant C^{(n)}_B$ with $C^{(n)}_B = m\ln_n[md/(d+m-1)]$ for $n \in (0,2]$. Here, $\ln_n(x) = (x^{1-n}-1)/(1-n)$, and $p^{(i)}_{ab}$ ($i = x, y, z$ and $a, b \in \{0,1\}$) rep-

TABLE IV. Experimental data of $S^B_{012}(\rho_{AB})/3$, $S^B_{12}(\rho_{AB})/2$, and $S^B_0(\rho_{AB})$ based on SIC.

θ	$S^B_{012}(\rho_{AB})/3$	$S^B_{12}(\rho_{AB})/2$	$S^B_0(\rho_{AB})$
0°	1.846 ± 0.036	1.849 ± 0.031	1.842 ± 0.047
10°	1.913 ± 0.077	2.011 ± 0.072	1.716 ± 0.089
20°	1.888 ± 0.075	2.273 ± 0.084	1.118 ± 0.058
30°	1.911 ± 0.078	2.624 ± 0.103	0.486 ± 0.028
40°	1.906 ± 0.071	2.831 ± 0.104	0.058 ± 0.006
45°	1.899 ± 0.092	2.849 ± 0.135	0.001 ± 0.007
50°	1.898 ± 0.092	2.819 ± 0.135	0.056 ± 0.006
60°	1.912 ± 0.070	2.627 ± 0.092	0.482 ± 0.025
70°	1.912 ± 0.058	2.304 ± 0.066	1.127 ± 0.044
80°	1.917 ± 0.065	2.018 ± 0.061	1.714 ± 0.073
90°	1.841 ± 0.026	1.848 ± 0.022	1.829 ± 0.035

TABLE V. The settings of HWP and QWP in the module (c) for realizing different PMOs on both Alice's photon and Bob's photon.

Settings	M^x_0	M^x_1	M^y_0	M^y_1	M^z_0	M^z_1
The angle of HWP	22.5°	−22.5°	22.5°	−22.5°	0°	45°
The angle of QWP	45°	45°	0°	0°	0°	0°

TABLE VI. Experimental data of LHS-SIGEUR for prepared Bell-like states.

θ	The LHS-SIGEUR for prepared Bell-like states
0°	1.002 ± 0.001
10°	0.887 ± 0.005
20°	0.592 ± 0.008
30°	0.253 ± 0.007
40°	0.034 ± 0.003
45°	0.004 ± 0.001
50°	0.033 ± 0.003
60°	0.255 ± 0.007
70°	0.591 ± 0.007
80°	0.888 ± 0.004
90°	1.003 ± 0.001

resents the probability of outcome (a, b) for a set of measurements $A_i \otimes B_i$ implemented on the photons of both Alice and Bob. $p_a^{(i)}$ is the probability of marginal outcome for measurement A_i of Alice. d is the dimension of the system, and m is the number of MUBs. In our experiment, $d = 2$, $m = 3$, and we choose $n = 2$ because the SIGEUR is the strongest one in this case [12,25,26]. Hence, the lower bound $C_B^{(n)} = 1$. In technology, we remove the module [Fig. 1(b)], and use module (c) to achieve the six PMOs performed on both Alice's photon and Bob's photon, as illuminated in Table V. Thereby, the steering inequality test can be implemented on all prepared Bell-like states. One can conveniently calculate $p_{ab}^{(i)}$ and $p_a^{(i)}$ according to the coincidence counts in experiment. The experimental left-hand sides of SIGEUR (LHS-SIGEUR) are shown in Fig. 5 and Table VI. The inset in Fig. 5 is the magnifications of the experimental results for Bell-like states with $\theta = 0°$ and $\theta = 90°$. It is experimentally demonstrated that the LHS-SIGEUR of nine prepared Bell-like states ($\theta = 10°, 20°, 30°, 40°, 45°, 50°, 60°, 70°, 80°$) can violate the SIGEUR (i.e., LHS-SIGEUR is less than 1). These experimental results further certify that the nine prepared Bell-like states are steerable states. Notably, the steerability of prepared Bell-like states with $\theta = 10°$ and $\theta = 80°$ (labeled by 1 and 2 in Fig. 5, respectively) can be observed by the SIGEUR. It further verifies that two setting coherence steering criterion based on SIC can indeed detect more steerable Bell-like states than the ones based on l_1C and REC.

IV. CONCLUSIONS

In this work, we experimentally demonstrate the complementarity relations between quantum steering criteria by employing prepared Bell-like states with high fidelity and three Pauli operators. The experimental results are in good accordance with the theoretical curves, and one can reveal the steerability of the system by detecting the average coherence of the subsystem. Whatever coherence measure is used, three measurement settings inequalities are always obeyed by all prepared Bell-like states in experiment. Meanwhile, the experimental $S_0^B(\rho_{AB})$ are anticorrelated with the $S_{12}^B(\rho_{AB})/2$. If the prepared Bell-like states violate two setting coherence steering criteria, then these states cannot violate one setting coherence steering criteria. Furthermore, the strengths of coherence steering criteria rely on the choice of coherence measure. In comparison with two setting coherence steering criteria based on l_1 norm of coherence and relative entropy of coherence, two setting coherence steering criterion based on skew information of coherence is most effective in witnessing two-photon steerable Bell-like states. From the perspective of experiment, the quantum coherence is an easily measurable quantity. Our experimental results imply that the quantum coherence as a resource can provide a useful tool to witness quantum steering in practical quantum information tasks. Also, our results demonstrate the connection between these two fundamental resources, namely, quantum coherence and quantum steering. These results may help us to investigate and understand the roles that these two resources play in quantum information and quantum thermodynamics.

ACKNOWLEDGMENTS

We would like to thank the reviewer for his/her guidance and help. This work was supported by the National Natural Science Foundation of China (Grants No. 11575001, No. 12004006, No. 11405171, No. 61601002, and No. 11605028), Anhui Provincial Natural Science Foundation (Grant No. 2008085QA43), the Program of Excellent Youth Talent Project of the Education Department of Anhui Province of China (Grants No. gxyq2018059, No. gxyqZD2019042, and No. gxyqZD2018065), the Natural Science Research Project of Education Department of Anhui Province of China (Grant No. KJ2018A0343), and the Open Foundation for CAS Key Laboratory of Quantum Information (Grants No. KQI201801 and No. KQI201804).

H.Y. and Z.-Y.D. contributed equally to this work.

[1] A. Einstein, B. Podolsky, and N. Rosen, Can quantum-mechanical description of physical reality be considered complete? Phys. Rev. **47**, 777 (1935).

[2] E. Schrödinger, Discussion of probability relations between separated systems, Math. Proc. Cambridge Philos. Soc. **31**, 555 (1935).

[3] R. Horodecki, P. Horodecki, M. Horodecki, and K. Horodecki, Quantum entanglement, Rev. Mod. Phys **81**, 865 (2009).

[4] J. S. Bell, On the Einstein Podolsky Rosen paradox, Physics **1**, 195 (1965).

[5] N. Brunner, D. Cavalcanti, S. Pironio, V. Scarani, and S. Wehner, Bell nonlocality, Rev. Mod. Phys. **86**, 419 (2014).

[6] H. M. Wiseman, S. J. Jones, and A. C. Doherty, Steering, Entanglement, Nonlocality, and the Einstein-Podolsky-Rosen Paradox, Phys. Rev. Lett. **98**, 140402 (2007).

[7] R. Uola, A. C. S. Costa, H. C. Nguyen, and O. Gühne, Quantum steering, Rev. Mod. Phys. **92**, 015001 (2020).

[8] E. G. Cavalcanti, S. J. Jones, H. M. Wiseman, and M. D. Reid, Experimental criteria for steering and the Einstein-Podolsky-Rosen paradox, Phys. Rev. A **80**, 032112 (2009).

[9] A. C. S. Costa and R. M. Angelo, Quantification of Einstein-Podolsky-Rosen steering for two-qubit states, Phys. Rev. A **93**, 020103(R) (2016).

[10] S. P. Walborn, A. Salles, R. M. Gomes, F. Toscano, and P. H. Souto Ribeiro, Revealing Hidden Einstein-Podolsky-Rosen Nonlocality, Phys. Rev. Lett. **106**, 130402 (2011).

[11] J. Schneeloch, C. J. Broadbent, S. P. Walborn, E. G. Cavalcanti, and J. C. Howell, Einstein-Podolsky-Rosen steering inequalities from entropic uncertainty relations, Phys. Rev. A **87**, 062103 (2013).

[12] A. C. S. Costa, R. Uola, and O. Gühne, Steering criteria from general entropic uncertainty relations, Phys. Rev. A **98**, 050104(R) (2018).

[13] T. Kriváchy, F. Fröwis, and N. Brunner, Tight steering inequalities from generalized entropic uncertainty relations, Phys. Rev. A **98**, 062111 (2018).

[14] M. Żukowski, A. Dutta, and Z. Yin, Geometric Bell-like inequalities for steering, Phys. Rev. A **91**, 032107 (2015).

[15] M. F. Pusey, Negativity and steering: A stronger Peres conjecture, Phys. Rev. A **88**, 032313 (2013).

[16] Y. Z. Zhen, Y. L. Zheng, W. F. Cao, L. Li, Z. B. Chen, N. L. Liu, and K. Chen, Certifying Einstein-Podolsky-Rosen steering via the local uncertainty principle, Phys. Rev. A **93**, 012108 (2016).

[17] D. J. Saunders, S. J. Jones, H. M. Wiseman, and G. J. Pryde, Experimental EPR-steering using Bell-local states, Nat. Phys. **6**, 845 (2010).

[18] D. H. Smith, G. Gillett, M. P. de Almeida, C. Branciard, A. Fedrizzi, T. J. Weinhold, A. Lita, B. Calkins, T. Gerrits, H. M. Wiseman, S. W. Nam, and A. G. White, Conclusive quantum steering with superconducting transition-edge sensors, Nat. Commun. **3**, 625 (2012).

[19] V. Händchen, T. Eberle, S. Steinlechner, A. Samblowski, T. Franz, R. F. Werner, and R. Schnabel, Observation of one-way Einstein-Podolsky-Rosen steering, Nat. Photonics **6**, 596 (2012).

[20] A. J. Bennet, D. A. Evans, D. J. Saunders, C. Branciard, E. G. Cavalcanti, H. M. Wiseman, and G. J. Pryde, Arbitrarily Loss-Tolerant Einstein-Podolsky-Rosen Steering Allowing a Demonstration over 1 km of Optical Fiber with No Detection Loophole, Phys. Rev. X **2**, 031003 (2012).

[21] S. Armstrong, M. Wang, R. Y. Teh, Q. Gong, Q. He, J. Janousek, H. A. Bachor, M. D. Reid, and P. K. Lam, Multipartite Einstein-Podolsky-Rosen steering and genuine tripartite entanglement with optical networks, Nat. Phys. **11**, 167 (2015).

[22] S. Wollmann, N. Walk, A. J. Bennet, H. M. Wiseman, and G. J. Pryde, Observation of Genuine One-Way Einstein-Podolsky-Rosen Steering, Phys. Rev. Lett. **116**, 160403 (2016).

[23] K. Sun, X. J. Ye, J. S. Xu, X. Y. Xu, J. S. Tang, Y. C. Wu, J. L. Chen, C. F. Li, and G. C. Guo, Experimental Quantification of Asymmetric Einstein-Podolsky-Rosen Steering, Phys. Rev. Lett. **116**, 160404 (2016).

[24] N. Tischler, F. Ghafari, T. J. Baker, S. Slussarenko, R. B. Patel, M. M. Weston, S. Wollmann, L. K. Shalm, V. B. Verma, S. W. Nam, H. C. Nguyen, H. M. Wiseman, and G. J. Pryde, Conclusive Experimental Demonstration of One-Way Einstein-Podolsky-Rosen Steering, Phys. Rev. Lett. **121**, 100401 (2018).

[25] S. Wollmann, R. Uola, and A. C. S. Costa, Experimental Demonstration of Robust Quantum Steering, Phys. Rev. Lett. **125**, 020404 (2020).

[26] H. Yang, Z.-Y. Ding, D. Wang, H. Yuan, X.-K. Song, J. Yang, C.-J. Zhang, and L. Ye, Experimental certification of the steering criterion based on a general entropic uncertainty relation, Phys. Rev. A **101**, 022324 (2020).

[27] A. Streltsov, G. Adesso, and M. Plenio, Quantum coherence as a resource, Rev. Mod. Phys. **89**, 041003 (2017).

[28] M. L. Hu, X. Y. Hu, J. C. Wang, Y. Peng, Y. R. Zhang, and H. Fan, Quantum coherence and geometric quantum discord, Phys. Rep. **762-764**, 1 (2018).

[29] T. Baumgratz, M. Cramer, and M. B. Plenio, Quantifying Coherence, Phys. Rev. Lett. **113**, 140401 (2014).

[30] C. Napoli, T. R. Bromley, M. Cianciaruso, M. Piani, N. Johnston, and G. Adesso, Robustness of Coherence: An Operational and Observable Measure of Quantum Coherence, Phys. Rev. Lett. **116**, 150502 (2016).

[31] M. Piani, M. Cianciaruso, T. R. Bromley, C. Napoli, N. Johnston, and G. Adesso, Robustness of asymmetry and coherence of quantum states, Phys. Rev. A **93**, 042107 (2016).

[32] S. Luo, Wigner-Yanase Skew Information and Uncertainty Relations, Phys. Rev. Lett. **91**, 180403 (2003).

[33] D. Girolami, Observable Measure of Quantum Coherence in Finite Dimensional Systems, Phys. Rev. Lett. **113**, 170401 (2014).

[34] C. S. Yu, Quantum coherence via skew information and its polygamy, Phys. Rev. A **95**, 042337 (2017).

[35] A. Streltsov, U. Singh, H. S. Dhar, M. N. Bera, and G. Adesso, Measuring Quantum Coherence with Entanglement, Phys. Rev. Lett. **115**, 020403 (2015).

[36] A. Winter and D. Yang, Operational Resource Theory of Coherence, Phys. Rev. Lett. **116**, 120404 (2016).

[37] T. R. Bromley, M. Cianciaruso, and G. Adesso, Frozen Quantum Coherence, Phys. Rev. Lett. **114**, 210401 (2015).

[38] T. Theurer, D. Egloff, L. Zhang, and M. B. Plenio, Quantifying Operations with an Application to Coherence, Phys. Rev. Lett. **122**, 190405 (2019).

[39] M.-L. Hu, Y.-Y. Gao, and H. Fan, Steered quantum coherence as a signature of quantum phase transitions in spin chains, Phys. Rev. A **101**, 032305 (2020).

[40] Y. Yao, X. Xiao, L. Ge, and C. P. Sun, Quantum coherence in multipartite systems, Phys. Rev. A **92**, 022112 (2015).

[41] K.-D. Wu, Z.-B. Hou, Y.-Y. Zhao, G.-Y. Xiang, C.-F. Li, G.-C. Guo, J.-J. Ma, Q.-Y. He, J. Thompson, and M. L. Gu, Experimental Cyclic Interconversion between Coherence and Quantum Correlations, Phys. Rev. Lett. **121**, 050401 (2018).

[42] W. Zheng, Z. Ma, H. Wang, S.-M. Fei, and X. Peng, Experimental Demonstration of Observability and Operability of Robustness of Coherence, Phys. Rev. Lett. **120**, 230504 (2018).

[43] A. Černoch, K. Bartkiewicz, K. Lemr, and J. Soubusta, Experimental tests of coherence and entanglement conservation under unitary evolutions, Phys. Rev. A **97**, 042305 (2018).

[44] Z.-Y. Ding, H. Yang, D. Wang, H. Yuan, J. Yang, and L. Ye, Experimental investigation of entropic uncertainty relations and coherence uncertainty relations, Phys. Rev. A **101**, 032101 (2020).

[45] N. Bohr, The quantum postulate and the recent development of atomic theory, Nature (London) **121**, 580 (1928).

[46] U. Singh, M. N. Bera, H. S. Dhar, and A. K. Pati, Maximally coherent mixed states: Complementarity between maximal coherence and mixedness, Phys. Rev. A **91**, 052115 (2015).

[47] S. Cheng and M. J. W. Hall, Complementarity relations for quantum coherence, Phys. Rev. A **92**, 042101 (2015).

[48] H.-H. Qin, S.-M. Fei, and X. Li-Jost, Trade-off relations of Bell violations among pairwise qubit systems, Phys. Rev. A **92**, 062339 (2015).

[49] G. Sharma and A. K. Pati, Trade-off relation for coherence and disturbance, Phys. Rev. A **97**, 062308 (2018).

[50] L.-J. Zhao, L. Chen, Y.-M. Guo, K. Wang, Y. Shen, and S.-M. Fei, Trade-off relation among genuine three-qubit nonlocalities in four-qubit systems, Phys. Rev. A **100**, 052107 (2019).

[51] D. Mondal, T. Pramanik, and A. K. Pati, Nonlocal advantage of quantum coherence, Phys. Rev. A **95**, 010301(R) (2017).

[52] F. Pan, L. Qiu, and Z. Liu, The complementarity relations of quantum coherence in quantum information processing, Sci. Rep. **7**, 43919 (2017).

[53] H. Zhu, Information complementarity: A new paradigm for decoding quantum incompatibility, Sci. Rep. **5**, 14317 (2015).

[54] X. Zhan, X. Zhang, J. Li, Y. Zhang, B. C. Sanders, and P. Xue, Realization of the Contextuality-Nonlocality Tradeoff with a Qubit-Qutrit Photon Pair, Phys. Rev. Lett. **116**, 090401 (2016).

[55] M. M. Weston, M. J. W. Hall, M. S. Palsson, H. M. Wiseman, and G. J. Pryde, Experimental Test of Universal Complementarity Relations, Phys. Rev. Lett. **110**, 220402 (2013).

[56] W.-M. Lv, C. Zhang, X.-M. Hu, H. Cao, J. Wang, and Y.-F. Huang, Experimental test of the trade-off relation for quantum coherence, Phys. Rev. A **98**, 062337 (2018).

[57] D. Mondal and D. Kaszlikowski, Complementarity relations between quantum steering criteria, Phys. Rev. A **98**, 052330 (2018).

[58] P. G. Kwiat, E. Waks, A. G. White, I. Appelbaum, and P. H. Eberhard, Ultrabright source of polarization-entangled photons, Phys. Rev. A **60**, R773 (1999).

[59] M. A. Nielsen and I. L. Chuang, *Quantum Computation and Quantum Information* (Cambridge University Press, Cambridge, 2000).

[60] J. B. Altepeter, E. R. Jeffrey, and P. G. Kwiat, Photonic state tomography, Adv. At., Mol., Opt. Phys. **52**, 105 (2005).

[61] D. F. V. James, P. G. Kwiat, W. J. Munro, and A. G. White, Measurement of qubits, Phys. Rev. A **64**, 052312 (2001).

[62] Z.-B. Hou, J.-F. Tang, C. Ferrie, G.-Y. Xiang, C.-F. Li, and G.-C. Guo, Experimental realization of self-guided quantum process tomography, Phys. Rev. A **101**, 022317 (2020).

[63] C. F. Li, J. S. Xu, X. Y. Xu, K. Li, and G. C. Guo, Experimental investigation of the entanglement-assisted entropic uncertainty principle, Nat. Phys. **7**, 752 (2011).